Hierarchical Assembly of Viral Nanotemplates with Encoded Microparticles via Nucleic Acid Hybridization

Wui Siew Tan,[†,§] Christina L. Lewis,[‡,§] Nicholas E. Horelik,[‡] Daniel C. Pregibon,[†] Patrick S. Doyle,*[,†] and Hyunmin Yi*[,‡]

Department of Chemical Engineering, Massachusetts Institute of Technology, Cambridge, Massachusetts 02139, and Department of Chemical and Biological Engineering, Tufts University, Medford, Massachusetts 02155

Received July 9, 2008. Revised Manuscript Received August 22, 2008

We demonstrate hierarchical assembly of tobacco mosaic virus (TMV)-based nanotemplates with hydrogel-based encoded microparticles via nucleic acid hybridization. TMV nanotemplates possess a highly defined structure and a genetically engineered high density thiol functionality. The encoded microparticles are produced in a high throughput microfluidic device via stop-flow lithography (SFL) and consist of spatially discrete regions containing encoded identity information, an internal control, and capture DNAs. For the hybridization-based assembly, partially disassembled TMVs were programmed with linker DNAs that contain sequences complementary to both the virus 5′ end and a selected capture DNA. Fluorescence microscopy, atomic force microscopy (AFM), and confocal microscopy results clearly indicate facile assembly of TMV nanotemplates onto microparticles with high spatial and sequence selectivity. We anticipate that our hybridization-based assembly strategy could be employed to create multifunctional viral-synthetic hybrid materials in a rapid and high-throughput manner. Additionally, we believe that these viral-synthetic hybrid microparticles may find broad applications in high capacity, multiplexed target sensing.

Introduction

Structurally and chemically complex hybrid materials are needed for high end applications in renewable energy, electronics, computing, diagnostics, medicine, and analytical chemistry.[1−6] To create materials with properties that transcend those of individual components, hierarchical assembly of units tailored across nanometer and micrometer length scales is highly desired.[7] Methods used to synthesize hierarchically assembled materials include direct or synergistic templating, self-assembly, photochemical patterning, electrodeposition, microcontact printing, and nanolithographic techniques.[7−9] These methods often involve a series of complex steps or have limited ability in controlling spatial resolution while maintaining full integrity of the individual components. Therefore, a facile method for hierarchically assembling hybrid materials under mild conditions in a selective manner is needed.

Recently, viruses have gained substantial attention as nanoscale templates for material synthesis.[10−18] They are structurally well defined, monodisperse, robust, nanoscaled units that have proven to be versatile substrates for the creation of novel materials by coupling to synthetic chemistry or genetic manipulation.[12,19−25] Site directed mutagenesis on viruses enables surface display of amino acids, which may be coupled to downstream chemical conjugation or used for direct display of peptides such as antibodies or enzymes in well defined spatial arrangements on the nanometer scale.[26−28] Tobacco mosaic virus (TMV) offers an attractive nanotemplate that provides high density covalent coupling sites with precise nanometer scale spacing. As shown in the atomic force microscopy (AFM) image of Figure 1b, a wild type TMV virion consists of approximately 2130 identical coat proteins helically wrapped around a 6.4 kb positive strand of genomic mRNA, making it an 18 nm diameter and 300 nm

* To whom correspondence should be addressed. Telephone: (617) 627-2195(H.Y.); (617) 253-4534 (P.S.D.). Fax: (617) 627-3991 (H.Y.); (617) 324-0066 (P.S.D.). E-mail: hyunmin.yi@tufts.edu (H.Y.); pdoyle@mit.edu (P.S.D.).

† Massachusetts Institute of Technology.

‡ Tufts University.

§ These authors contributed equally to this work.

(1) Chomski, E.; Ozin, G. *Adv. Mater.* **2000**, *12*, 1071–1078.

(2) Correia, A.; Perez, M.; Saenz, J. J.; Serena, P. A. *Phys. Status Solidi A* **2007**, *204*, 1611–1622.

(3) Lehn, J.-M. *Science* **2002**, *295*, 2400–2403.

(4) Ozin, G. A. *Chem. Commun.* **2000**, 419–432.

(5) Ungar, G.; Liu, Y.; Zeng, X.; Percec, V.; Cho, W.-D. *Science* **2003**, *299*, 1208–1211.

(6) Zuo, L.; Wei, W.; Morris, M.; Wei, J.; Gorbounov, M.; Wei, C. *Med. Clin. North Am.* **2007**, *91*, 845.

(7) Whitesides, G. M.; Grzybowski, B. *Science* **2002**, *295*, 2418–2421.

(8) Lakes, R. *Nature* **1993**, *361*, 511–515.

(9) Sanchez, C.; Arribart, H.; Giraud Guille, M. M. *Nat. Mater.* **2005**, *4*, 277–288.

(10) Dujardin, E.; Peet, C.; Stubbs, G.; Culver, J. N.; Mann, S. *Nano Lett.* **2003**, *3*, 413–417.

(11) Fowler, C. E.; Shenton, W.; Stubbs, G.; Mann, S. *Adv. Mater.* **2001**, *13*, 1266–1269.

(12) Lee, L. A.; Wang, Q. *Nanomedicine* **2006**, *2*, 137.

(13) Niu, Z. W.; Bruckman, M. A.; Li, S. Q.; Lee, L. A.; Lee, B.; Pingali, S. V.; Thiyagarajan, P.; Wang, Q. *Langmuir* **2007**, *23*, 6719–6724.

(14) Balci, S.; Noda, K.; Bittner, A. M.; Kadri, A.; Wege, C.; Jeske, H.; Kern, K. *Angew. Chem., Int. Ed.* **2007**, *46*, 3149–3151.

(15) Huang, Y.; Chiang, C. Y.; Lee, S. K.; Gao, Y.; Hu, E. L.; Yoreo, J. D.; Belcher, A. M. *Nano Lett.* **2005**, *5*, 1429–1434.

(16) Yoo, P. J.; Nam, K. T.; Qi, J.; Lee, S.-K.; Park, J.; Belcher, A. M.; Hammond, P. T. *Nat. Mater.* **2006**, *5*, 234.

(17) Chiang, C. Y.; Mello, C. M.; Gu, J.; Silva, E.; Van Vliet, K.; Belcher, A. *Adv. Mater.* **2007**, *19*, 826–832.

(18) Steinmetz, N. F.; Findlay, K. C.; Noel, T. R.; Parker, R.; Lomonossoff, G. P.; Evans, D. J. *ChemBioChem* **2008**, *9*, 1662–1670.

(19) Fischlechner, M.; Donath, E. *Angew. Chem., Int. Ed.* **2007**, *46*, 3184–3193.

(20) Fischlechner, M.; Toellner, L.; Messner, P.; Grabherr, R.; Donath, E. *Angew. Chem., Int. Ed.* **2006**, *45*, 784–789.

(21) Douglas, T.; Young, M. *Adv. Mater.* **1999**, *11*, 679–310.

(22) Manchester, M.; Singh, P. *Adv. Drug Delivery Rev.* **2006**, *58*, 1505.

(23) Merzlyak, A.; Lee, S.-W. *Curr. Opin. Chem. Biol.* **2006**, *10*, 246.

(24) Singh, P.; Gonzalez, M. J.; Manchester, M. *Drug Dev. Res.* **2006**, *67*, 23–41.

(25) Gazit, E. *FEBS J.* **2007**, *274*, 317–322.

(26) Smolenska, L.; Roberts, I. M.; Learmonth, D.; Porter, A. J.; Harris, W. J.; Wilson, T. M. A.; Santa Cruz, S. *FEBS Lett.* **1998**, *441*, 379.

(27) Schwyzer, R.; Kriwaczek, V. M. *Biopolymers* **1981**, *20*, 2011–2020.

(28) Werner, S.; Marillonnet, S.; Hause, G.; Klimyuk, V.; Gleba, Y. *Proc. Natl. Acad. Sci. U.S.A.* **2006**, *103*, 17678–17683.

10.1021/la802089q CCC: $40.75
Published on Web 10/04/2008

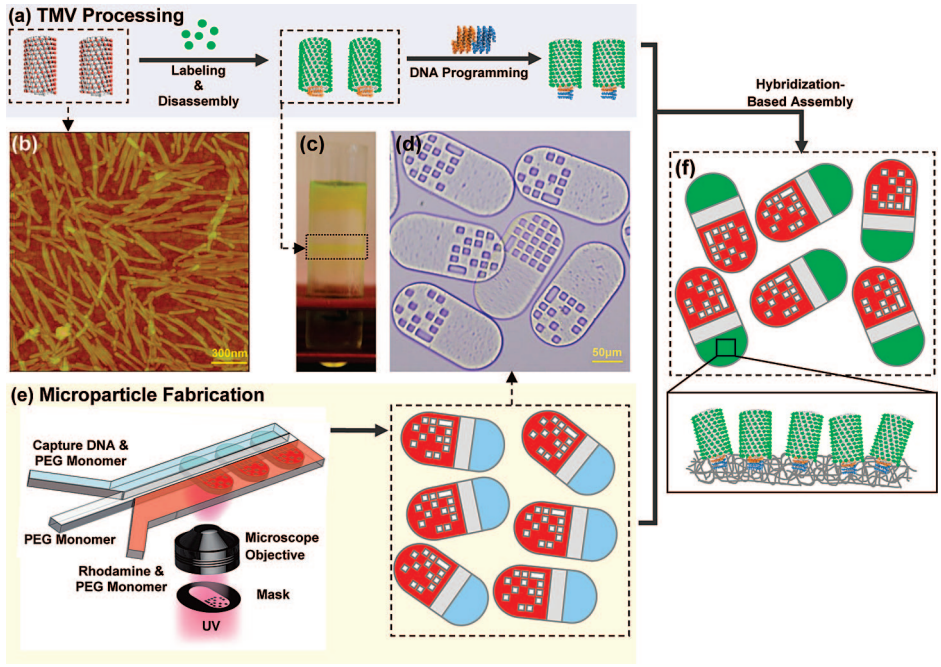

Figure 1. Hierarchical assembly of fluorescein-labeled TMV1cys nanotemplates onto encoded and capture DNA embedded PEG-based microparticles. (a) Schematic diagram depicting the labeling, disassembly, and programming of TMV1cys. The TMV models are generated from UCSF Chimera software (Experimental Section) and represent approximately one tenth of the total TMV virion. The red dots represent cysteine residues genetically displayed on the outer surface of each coat protein (~2130 identical proteins per virion), adding precisely spaced thiol functionality for covalent conjugation of fluorescent markers. Partial disassembly followed by hybridization with linker DNA confers capture DNA sequence-specific assembly address. (b) AFM topographical image of TMV1cys. The yellow bar represents 300 nm. (c) Sucrose gradient containing fluorescently labeled TMVs as a discrete band (boxed) separated from unreacted fluorescein dye at the top of the sucrose gradient. (d) Brightfield micrograph of encoded microparticles. The yellow bar represents 50 μm. (e) Schematic diagram of stop-flow lithography (SFL) for production of encoded and DNA embedded microparticles. (f) Formation of nanobio-synthetic hybrid microentities following hybridization-based assembly of TMVs with microparticles.

long rigid nanotube with a 4 nm diameter inner channel.[29] Particularly, TMV possesses several unique properties as nanotemplates such as simple mass production,[30] a well defined structure,[29,31−33] and extraordinary stability. For example, TMV has been shown to be stable under various harsh conditions: temperatures up to 90 °C, extreme pHs (2−10), and organic solvents (80% ethanol, methanol, and DMSO).[30,34,35] Furthermore, the ability to confer surface functionalities via genetic manipulation[36] makes TMV an attractive choice compared to inorganic nanotubes. TMV has thus been exploited in creating a wide range of organic-inorganic hybrid materials[37,38] and has also been applied in functional digital memory devices[39] and battery electrodes.[40] Therefore, patterned assembly of TMVs[41,42] in a hierarchical manner would provide means to fully harness TMV's unique potential as a nanotemplate.

We have previously demonstrated continuous fabrication of poly(ethylene glycol) (PEG)-based microparticles with custom designed geometries and tunable chemical anisotropy via stop-flow lithography (SFL).[43] Benefits of the SFL technique include rapid and continuous production of monodisperse and biocompatible microparticles in a high throughput manner. This simple microfluidic technique affords the ability to create microparticles consisting of spatially discrete regions containing encoded identity information and covalently attached capture DNAs. The encoded region may be used to distinguish the microparticles from one another with over a million different codes available, allowing immense multiplexing capability.[44] The region containing covalently attached capture DNAs provides a platform for selectively patterning TMV. Combining the two technologies of TMV nanotemplates and encoded microparticles to create multifaceted hybrid materials may have significant potential in a broad range of applications including high throughput sensing.

In this paper, we demonstrate hierarchical assembly of fluorescein-labeled TMV1cys nanotemplates onto encoded microparticles, as shown in Figure 1. As shown in the schematic diagram of Figure 1a, genetically modified TMV1cys nanotemplates possess one cysteine residue on the outer surface of each coat protein that serves as a covalent coupling site for fluorescein-maleimide, a fluorescein derivative that forms a covalent thioether linkage with cysteine's thiol group.[41,42] These labeled TMVs were then partially disassembled to expose the 5′ end genomic RNA via sucrose gradient ultracentrifugation under alkaline pH. Since coat protein-RNA interactions are weakest at the 5′ end of the viral RNA, mild alkaline treatments and centrifugation

(29) Culver, J. N. *Annu. Rev. Phytopathol.* **2002**, *40*, 287–310.
(30) Zaitlin, M. *AAB Descriptions of Plant Viruses* **2000**, 370.
(31) Klug, A. *Philos. Trans. R. Soc. London, Ser. B* **1999**, *354*, 531–535.
(32) Lebeurier, G.; Nicolaieff, A.; Richards, K. E. *Proc. Natl. Acad. Sci. U.S.A.* **1977**, *74*, 149–153.
(33) Namba, K.; Stubbs, G. *Science* **1986**, *231*, 1401–1406.
(34) Knez, M.; Sumser, M.; Bittner, A. M.; Wege, C.; Jeske, H.; Martin, T. P.; Kern, K. *Adv. Funct. Mater.* **2004**, *14*, 116–124.
(35) Stubbs, G. *Semin. Virol.* **1990**, *1*, 405–412.
(36) Dawson, W. O.; Beck, D. L.; Knorr, D. A.; Grantham, G. L. *Proc. Natl. Acad. Sci. U.S.A.* **1986**, *83*, 1832–1836.
(37) Liu, W. L.; Alim, K.; Balandin, A. A.; Mathews, D. M.; Dodds, J. A. *Appl. Phys. Lett.* **2005**, *86*, 253108-3.
(38) Fonoberov, V. A.; Balandin, A. A. *Nano Lett.* **2005**, *5*, 1920–1923.
(39) Tseng, R. J.; Tsai, C.; Ma, L.; Ouyang, J.; Ozkan, C. S.; Yang, Y. *Nat. Nanotechnol.* **2006**, *1*, 72–77.
(40) Royston, E.; Ghosh, A.; Kofinas, P.; Harris, M. T.; Culver, J. N. *Langmuir* **2008**, *24*, 906–912.
(41) Yi, H.; Rubloff, G. W.; Culver, J. N. *Langmuir* **2007**, *23*, 2663–2667.
(42) Yi, H. M.; Nisar, S.; Lee, S. Y.; Powers, M. A.; Bentley, W. E.; Payne, G. F.; Ghodssi, R.; Rubloff, G. W.; Harris, M. T.; Culver, J. N. *Nano Lett.* **2005**, *5*, 1931–1936.
(43) Dendukuri, D.; Gu, S. S.; Pregibon, D. C.; Hatton, T. A.; Doyle, P. S. *Lab Chip* **2007**, *7*, 818–828.
(44) Pregibon, D.; Toner, M.; Doyle, P. S. *Science* **2007**, *315*, 1393–1396.

Table 1. Single Stranded DNA Sequences

Name	5'end	Sequence	3'end
Capture DNA Embedded within the Microparticles			
C1	Acrydite-C18	ATGATGATGATGATGATG	---
C2	Acrydite-C18	TTTTTCGGCAGGTCGGTAAC	---
C3	Acrydite-C18	CACTACCGATACGTACTCAG	---
Fluorescently Labeled Single Stranded DNA Hybridized with Microparticles			
C3'	FITC[1]	CTGAGTACGTATCGGTAGTG	---
Linker DNA Hybridized with TMV and Microparticles			
C2'	---	GTTTGTTGTTGTTGGTAATTGTTG*TTTTT*GTTACCGACCTGCCGAAAAA[2]	---

1. FITC: fluorescein isothiocyanate.

2. The detailed sequence description entails: TMV 5'end Complementary Sequence *Spacer* Address-specific Sequence.

can be used to mimic cellular conditions in order to partially disassemble the virus and expose the 5′ end of its genome.[42] Figure 1c shows that these fluorescently labeled TMVs form a discrete band while unreacted fluorescein dye remains at the top of the sucrose gradient. Next, these TMVs were programmed via hybridization with linker DNA consisting of two regions: one complementary to TMV's 5′ end RNA and the other complementary to the microparticle's capture DNA sequence. This confers the capture DNA sequence-specific assembly address to the TMV (Table 1).

The PEG-based microparticles consisting of the encoded, control, and capture DNA regions were fabricated in a microfluidic device via SFL, as shown in the schematic diagram of Figure 1e. The regions of different functionality are copolymerized seamlessly within each microparticle by a single UV exposure through a photomask with the desired microparticle shape. This photolithography-based microfluidic technique of SFL enables rapid and continuous production of various shaped microparticles using diacrylate chemistry and patterned UV cross-linking through a photomask containing the desired microparticle shape. A brightfield micrograph of these microparticles is shown in Figure 1d. Hybridization-based assembly of the labeled and programmed TMVs with the encoded microparticles containing capture DNA creates nanobio-synthetic hybrid microentities, as shown in Figure 1f. Fluorescence microscopy, AFM, and confocal microscopy results clearly illustrate facile assembly of TMV nanotemplates onto microparticles with high spatial and sequence selectivity. Since proteins and antibodies can be covalently linked to TMV via its high density thiol surface functionality, we envision that our facile assembly strategy can be readily exploited for a variety of biotechnological applications such as high throughput, multiplexed protein sensing.[45,46]

Experimental Section

TMV1cys and Fluorescent Labeling. TMV1cys was provided as a generous gift from Dr. James Culver, University of Maryland Biotechnology Institute, Center for Biosystems Research. Purified TMV1cys was incubated at room temperature for 2 h with 10-fold molar excess of fluorescein-5-maleimide (Biotium, Hayward, CA) in 100 mM Tris buffer, pH 7.0. The fluorescein-labeled virus was separated by centrifugation in a 10−40% sucrose gradient[41,42] at 48 000*g* for 2 h while the pH was adjusted to 8.0 to partially remove coat protein subunits from the 5′ ends of the viral genome. Partially disassembled virions were pelleted by centrifugation for 40 min at 106 000*g*. Pelleted viruses were resuspended in 5× SSC buffer (75 mM sodium citrate, 750 mM sodium chloride, pH 7.0).

Microparticle Fabrication. PEG microparticles were synthesized as previously described.[44] Briefly, a poly(ethylene glycol) diacrylate (PEG-DA, M_n = 700, Aldrich) monomer was mixed with 2.5 vol % 2-hydroxy-2-methylpropiophenone photoinitiator (Darocure 1173, Aldrich) and 33 vol % TE buffer (10 mM Tris, pH 8.0 (Rockland Immunochemicals, Inc., Gilbertsville, PA) and 1 mM EDTA (OmniPur)) containing 0.01 vol % of 10 wt % sodium dodecyl sulfate (SDS, Invitrogen). This base monomer mixture was in turn mixed in a 9:1 volume ratio with 1 part of TE solution containing DNA−Acrydite capture DNAs, blue food dye (to visualize the coflowing monomer streams using bright-field microscopy), or Rhodamine B (Polysciences Inc., Warrington, PA). DNA probes (IDT Technologies, Coralville, IA) were modified with a reactive Acrydite group and an 18-carbon spacer. Three different capture DNA sequences were used in this study as shown in Table 1. Final prepolymer mixtures contained either (a) 50 μM DNA−Acrydite capture DNA (C1, C2, or C3), (b) 1 vol % blue food dye, or (c) 0.1 mg/mL Rhodamine B. The prepolymer mixtures were coflowed through microfluidic poly(dimethylsiloxane) (PDMS) devices made by traditional soft lithographic methods. Channels were designed with one to three 100 μm wide channels that converged into a single 200−400 μm wide channel allowing coflow of up to three different monomer streams to create microparticles with up to three distinct regions. The thickness of each stream was controlled by adjusting the relative pressure on each of the inlet channels, which were connected to a pressure source (regulated by a pressure valve, Controlair Inc., Amherst, NH). Using an inverted Zeiss Axiovert 200 microscope with a 100 W HBO mercury lamp and photomasks inserted in the field-stop position, PEG microparticles were polymerized by 75 ms bursts of wide-excitation ultraviolet (UV) light from a 11000v2 UV filter set (Chroma Technology Corp., Rockingham, VT). A computerized stop-polymerize-flow sequence of ∼1 s was cycled to obtain thousands of microparticles in less than 20 min. The resulting microparticles were 30 μm thick and of shapes projected from the photomask. Using a 20× optical objective, photomasks were designed to form the180 μm × 90 μm encoded microparticles shown in Figure 1d. These microparticles (three types) were made using three coflowed streams, shown in Figure 1e with capture DNA C1, C2, or C3, each containing a different encoded region. Microparticles were cleaned of unreacted monomer with three different rinse solutions: TE buffer containing 0.1% Tween 20

(45) Sapsford, K. E.; Soto, C. M.; Blum, A. S.; Chatterji, A.; Lin, T.; Johnson, J. E.; Ligler, F. S.; Ratna, B. R. *Biosens. Bioelectron.* **2006**, *21*, 1668–1673.
(46) Scheck, R. A.; Francis, M. B. *ACS Chem. Biol.* **2007**, *2*, 247–251.

surfactant, PEG-DA monomer, and TE buffer containing 1% Tween 20 surfactant. The rinses were completed with ~1 mL of rinse solution, vortexing, centrifugation, and aspiration of supernatant. Microparticles were stored in TE buffer containing 1% Tween 20 surfactant at 20 °C before use in hybridizations.

Hybridization-Based Assembly of TMV Nanotemplates. For address-specific programming of labeled and partially disassembled TMV, 10-fold molar excess of linker DNA (IDT Technologies, Coralville, IA) was added to fluorescein-labeled TMV solutions and incubated at 30 °C for 2 h. The linker DNA consisted of two regions: one complementary to TMV's 5′ end RNA and the other complementary to the microparticle's capture DNA sequence, as shown in Table 1. To remove the unbound linker DNA, mixtures were centrifuged at 106 000*g* for 40 min in 5× SSC buffer. The fluorescein-labeled single stranded (ss) DNA, described in Table 1, was purchased from Gene Probe Technologies Inc. (Gaithersburg, MD). For assembly of TMV, fluorescein-labeled ssDNA, and microparticles, both the programmed TMV pellets and fluorescein-labeled ssDNA were resuspended in 5× SSC buffer containing 0.01% Tween 20 and hybridized with the microparticles overnight at 37 °C. The final TMV and ssDNA concentrations in the hybridization solution were ~50−100 nM. The microparticles were then rinsed several times with 2× SSC buffer containing 0.01% Tween 20.

Analysis. The hybridized miroparticles were visualized using standard filter sets U-N31001 and U-N31002 (Chroma Technology Corp., Rockingham, VT), compatible with fluorescein and rhodamine fluorophores, respectively, in an Olympus BX51 microscope. Still images were captured using a DP70 microscope digital camera. The fluorescence images were evaluated with the fluorescence intensity profile function from ImageJ software (http://rsb.info.nih.gov/ij/). AFM images were obtained using a Dimension 3100 atomic force microscope (Digital Instruments, Santa Barbara, CA) with a Nanoscope IV controller operated in dry tapping mode with a scan rate of 0.5 Hz and moderate amplitude setpoints. Tap300 silicon probes (Budget Sensors, Sofia, Bulgaria) were used at approximately 300 Hz. The AFM images were analyzed using Nanoscope software version 6.00. Confocal images were acquired on a Leica DMIRE2 microscope with a TCS SP2 scanner (Wetzlar, Germany). The system was equipped with a 63× (NA 1.2) water immersion objective, which was used in this study. Samples were placed on number 1.5 cover glass within a PDMS well and excited at 488 nm. Fluorescence emission spectra were detected from 500 to 530 nm. The depth scan increment was 1 μm with a scan thickness of ~155 nm. Analysis was performed with the Leica Confocal software (Wetzlar, Germany).

Molecular Modeling. The TMV molecular graphics images were produced using the UCSF Chimera package (http://www.cgl.ucsf.edu/chimera)[47−49] from the Resource for Biocomputing, Visualization, and Informatics at the University of California, San Francisco (supported by NIH P41 RR-01081). The base structure of TMV (PDB ID: 2tmv)[50] used in the molecular graphics images was obtained from the Research Collaboratory for Structural Bioinformatics Protein Data Bank (RCSB PDB, http://www.pdb.org/).[51]

Results and Discussion

Hierarchical Assembly of TMV Nanotemplates with Encoded Microparticles. As shown in Figure 2, we first demonstrate hierarchical assembly of fluorescein-labeled TMV1cys nanotemplates onto microparticles via nucleic acid hybridization. The microparticles were fabricated in a microfluidic device via stop-flow lithography (SFL),[43] as shown in Figure 1e, and they consist of three discrete regions: an encoded region containing Rhodamine B, a middle negative control region, and a capture DNA region. TMV1cys nanotemplates were labeled with fluorescein maleimide, which forms a covalent thioether bond with the genetically displayed cysteine's thiol groups. These labeled TMVs were partially disassembled to expose the 5′ end genomic RNA and then programmed with linker DNAs via hybridization to confer the capture DNA sequence-specific address. These labeled and programmed TMVs were incubated with microparticles for hybridization-based assembly and examined with a fluorescence microscope, as shown in Figure 2.

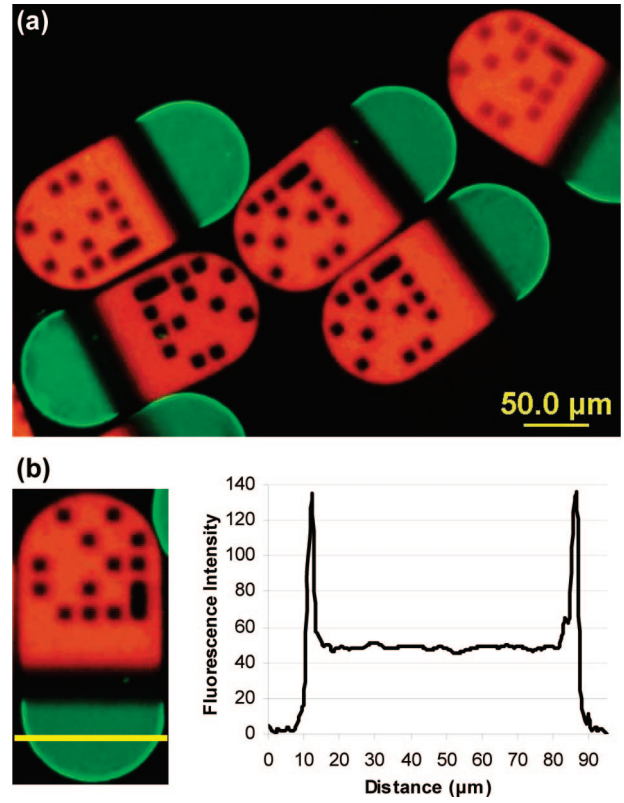

Figure 2. Hierarchical assembly of fluorescein-labeled TMV1cys nanotemplates onto microparticles via nucleic acid hybridization. (a) Overlay fluorescence image of fluorescein-labeled TMV1cys onto Rhodamine B labeled and encoded microparticles. Three regions define the 180 μm × 90 μm × 30 μm microparticles: an encoded region containing Rhodamine B, a middle negative control region, and a capture DNA region. (b) Fluorescence intensity plot across the TMV-assembled region shown by the yellow line.

As shown in the fluorescence micrograph of Figure 2a, fluorescein-labeled TMVs readily assembled onto the capture DNA region of the microparticles. Importantly, the encoded and middle control regions of the microparticles showed minimal nonspecific binding (from TMV1cys-conjugated fluorescein), demonstrating high spatial selectivity. Figure 2a also shows the reproducibility of both the particle fabrication process and TMV1cys assembly. The fluorescence intensity profile plot in Figure 2b shows a uniform TMV assembly density on the microparticles, as the fluorescence intensity is nearly constant across the TMV region of the microparticles, excluding the edges. Since the TMVs are unable to penetrate far into the microparticles, their localization near the surface of the capture DNA region is expected and results in the bright edges seen when microparticles are lying flat and viewed top-down as shown in Figure 2a. Combined, these results demonstrate the highly uniform and multifunctional nature of the microparticles, and the creation of viral-synthetic microentities via hybridization-based assembly of TMV nanotemplates with encoded microparticles.

(47) Pettersen, E. F.; Goddard, T. D.; Huang, C. C.; Couch, G. S.; Greenblatt, D. M.; Meng, E. C.; Ferrin, T. E. *J. Comput. Chem.* **2004**, *25*, 1605–1612.
(48) Couch, G. S.; Hendrix, D. K.; Ferrin, T. E. *Nucleic Acids Res.* **2006**, *34*, e29.
(49) Goddard, T. D.; Huang, C. C.; Ferrin, T. E. *Structure* **2005**, *13*, 473–482.
(50) Namba, K.; Pattanayek, R.; Stubbs, G. *J. Mol. Biol.* **1989**, *208*, 307–325.
(51) Berman, H. M.; Westbrook, J.; Feng, Z.; Gilliland, G.; Bhat, T. N.; Weissig, H.; Shindyalov, I. N.; Bourne, P. E. *Nucleic Acids Res.* **2000**, *28*, 235–242.

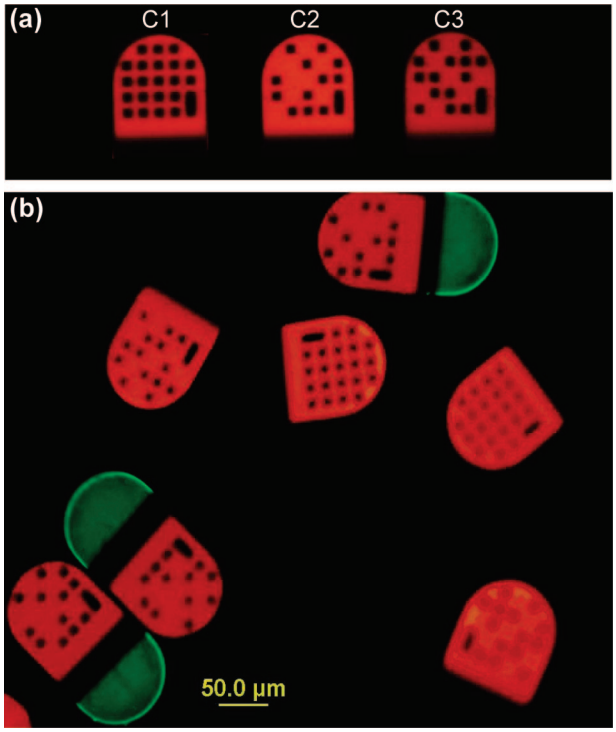

Figure 3. TMV templates hybridized with a mixture of three different microparticle types. (a) Three microparticle types, all differing by the barcode and capture DNA sequence embedded within the microparticles. (b) Fluorescence overlay image showing fluorescein-labeled TMV1cys assembled onto only the microparticles containing the matching DNA sequence, C2.

Sequence-Specific Assembly of TMV with Multiple Microparticle Types. To directly demonstrate the sequence specificity of our assembly procedure, we incubated the fluorescein-labeled and linker DNA (C2′) programmed TMV1cys nanotemplates with a mixture of microparticles, as shown in Figure 3. This microparticle mixture contained three types, as shown in Figure 3a, each with different codes and capture DNA sequences (C1, C2, and C3). The fluorescence micrograph of Figure 3b clearly shows that TMVs assembled only onto the microparticles containing the matching capture DNA sequence (C2). Importantly, minimal fluorescence in the capture DNA area of the nonspecific microparticles demonstrates the highly selective nature of the hybridization-based assembly. This result confirms that the assembly event occurs via sequence-specific hybridization, suggesting the feasibility of simultaneous "one-pot" assembly of multiple TMV conjugates with a large number of microparticle types, each containing a different barcode and capture DNA sequence. Additionally, the encoded region enables identification of the DNA sequence derived functionality, suggesting the potential for a high throughput screening capability. Similarly, site-specific assembly of TMV conjugates carrying multiple functionalities to multiple regions on a single particle could also be envisioned. The latter could readily be achieved using the versatility of the SFL process that allows production of microparticles with more than one DNA capture region containing different capture DNA sequences.

Atomic Force Microscopy (AFM) of TMV Nanotemplates on Microparticles. AFM has been extensively employed in studying biological materials, especially TMVs on solid substrates. These efforts have led to the elucidation of various fundamental properties including mechanical strengths,[52] conductivity,[39] and flexoelectricity[53] to list a few. Here, we have used AFM to physically confirm the presence of TMV nanotemplates on the microparticles and examine the structural integrity of assembled TMVs. For this, the TMV-assembled microparticles were extensively rinsed, dried under ambient conditions for 5 days, and examined in the tapping mode using a standard silicon tip. The phase contrast AFM image of Figure

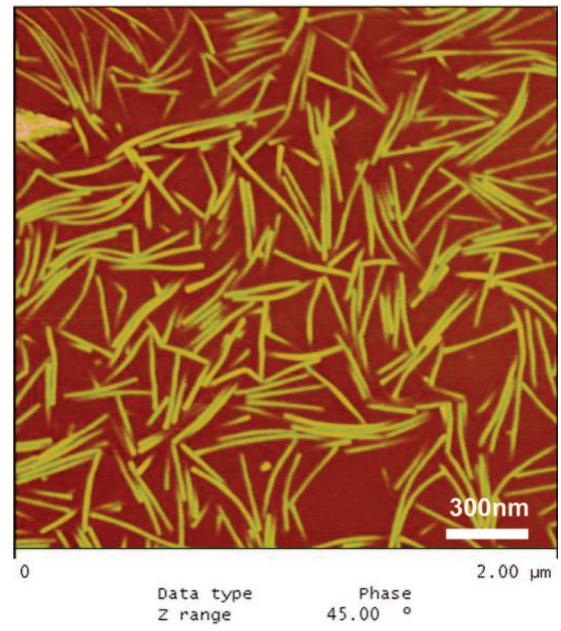

Figure 4. AFM phase contrast image of TMV assembled onto encoded microparticles.

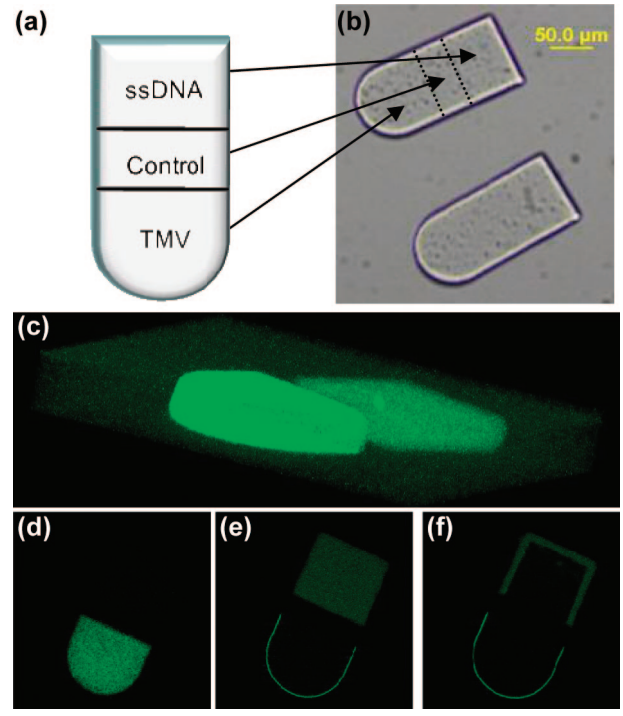

Figure 5. One-pot assembly of fluorescein-labeled TMV and ssDNA onto discrete regions of multifunctional microparticles. (a) Schematic diagram showing the three regions of the multifunctional microparticles: the TMV complementary (round edge) and ssDNA complementary (straight edge) regions are separated by a middle negative control region. (b) Brightfield image of the multifunctional microparticles. The yellow bar represents 50 μm. (c) Reconstituted 3-D confocal image of a multifunctional microparticle following hybridization with the fluorescein-labeled TMV and ssDNA. (d−f) Confocal z-scan images of TMV and ssDNA hybridized microparticles at the surface (d), several micrometers below the surface (e), and center (f).

4 clearly shows that TMV1cys nanotemplates are assembled on the microparticles with high density and full structural integrity. Further, the encoded and negative control regions were also examined via AFM and did not show a significant number of TMVs (images not shown). Additionally, despite the extensive rinsing and drying conditions necessary for AFM sample preparation, the microparticle-assembled TMVs retained their structure, demonstrating the stability of these hybridized TMV1cys nanotemplates. Overall, this result clearly confirms the presence and structural integrity of TMV nanotemplates assembled on microparticles.

Confocal Microscopy of TMV-Assembled Microparticles. As shown in Figure 5, we employed confocal microscopy to examine detailed 3-D assembly features of the TMV- and fluorescein-labeled ssDNA-assembled microparticles. As shown in the schematic diagram (a) and the brightfield micrograph (b), the microparticles used for this evaluation contained two spatially discrete capture DNA regions coding different sequences and separated by a negative control region. These microparticles were incubated in a solution containing two fluorescein-labeled species: fluorescein-labeled TMV programmed with linker DNA complementary to the round region (C2) and fluorescein-labeled ssDNA complementary to the rectangular region (C3).

A *z*-scan analysis on these microparticles clearly shows the difference in the 3-D assembly feature between the two regions, as shown in Figure 5c−f. First, the three-dimensional reconstituted image of Figure 5c shows the difference in spatially selective assembly and in material characteristics between the TMV-assembled and DNA-assembled regions. The TMV-assembled region shows bright fluorescence at the very outer surface of the microparticles and minimal fluorescence within the microparticle volume (see also a movie in the Supporting Information). This is likely due to the large size of the TMV that prevents deep penetration into the hydrogel matrix of the particle. In contrast, the DNA-assembled region shows more dispersed fluorescence near the particle surface. This is likely due to the smaller size of the fluorescein-labeled DNA that allows it to diffuse further into the hydrogel and correlates well with our previously reported results.[44] This difference in the penetration depth is further demonstrated in the *z*-scan images of Figure 5 at the surface (d), several micrometers below the surface (e), and at the center (f). Figure 5d, taken at the top surface of the microparticle, shows that TMVs are assembled only onto the circular region with high fluorescence intensity, while the rectangular ssDNA region shows minimal fluorescence. As the *z*-scan layer moves a few micrometers toward the microparticle center, Figure 5e shows that the TMV layer is confined to the very outer surface whereas the fluorescein-labeled DNA layer just starts to appear. Finally, Figure 5f, taken at the microparticle center, shows that the TMVs are mainly assembled within the outer $\sim 2\ \mu$m region of the microparticles with high fluorescence while DNA penetrates several micrometers deeper. Importantly, these confocal microscopy results illustrate the high fluorescein-templating density of the TMV nanotemplates given the same fabrication condition and thus capture DNA density in the two regions. The difference in fluorescence intensities of the TMV bound region versus the ssDNA bound region reflects the high fluorescein-templating density of the TMV nanotemplates. Since numerous fluorescein molecules are conjugated to each TMV while only one fluorescein molecule is attached to each ssDNA, the amount of fluorescence prior to DNA binding even is multifold for TMV compared to ssDNA. Furthermore, the two capture DNA regions do not show any overlapping assembly characteristics, strongly suggesting the sequence specificity of the sequence design and assembly procedures. Together, these results illustrate the potential for integrating TMVs and SFL in creating multifaceted hybrid materials.

Conclusion

Hierarchically assembled materials structured across nano- and micrometer length scales provide the ability to exploit features on submicrometer scales in macroscopic devices as well as form materials with new properties tailored for specific applications. A major challenge among the current methods for creating hierarchically assembled materials is the limited ability in controlling spatial resolution while maintaining full integrity of the individual components. Thus, a facile method for hierarchically assembling hybrid materials under mild conditions in a spatially selective manner is needed.

The fluorescence microscopy results reported in this study illustrated both the spatially selective and sequence-specific nature of the assembly process. High spatial selectivity is afforded by the fidelity of the sequence-specific DNA hybridization used in our assembly process and holds potential for one-pot assembly of multiple TMV conjugates to different encoded microparticles or to different regions on a single microparticle. In addition, the assembly and particle fabrication processes were shown to be very reproducible. The AFM images clearly showed that the TMV nanotemplates are assembled on the microparticles with high density and full structural integrity despite the extensive rinsing and drying required to prepare samples for AFM analysis. The confocal microscopy results demonstrated the feasibility of one-pot assembly between multiple TMV conjugates and a large number of microparticle types, each containing a different barcode and capture DNA sequence. The confocal microscopy images also showed the high fluorescein-templating density of the TMV nanotemplates and that these nanotemplates are assembled on the microparticle surface. Combined, these results represent a novel high throughput route to create multiplexed and multifunctional viral-synthetic hybrid microentities in mild aqueous conditions. We expect that the integration of viral nanotemplates and the rapid SFL technique will have significant potential in creating complex structures for a broad range of applications. For example, one could envision protein sensing with antibody-conjugated TMVs assembled onto encoded microparticles. The multiplexing capability of such protein-viral-synthetic hybrid materials would enable high throughput analysis of analytes.[44]

Acknowledgment. We thank Dr. James Culver at the University of Maryland Biotechnology Institute, Center for Biosystems Research, for providing the generous gift of TMV1cys. We also thank Jonathan Levitt at Tufts University, Biomedical Engineering Department, for assistance with the confocal microscopy analysis. This work was supported in part by a Tufts Faculty Research Award (FRAC, H.Y.) and by NSF Grant CTS-0304128 (P.S.D.).

Supporting Information Available: Movie of the 3-D confocal reconstruction image of a multifunctional microparticle hybridized with fluorescein-labeled TMV and ssDNA. This material is available free of charge via the Internet at http://pubs.acs.org.

LA802089Q

(52) Schmatulla, A.; Maghelli, N.; Marti, O. *J. Microsc. (Oxford)* **2007**, *225*, 264–268.

(53) Kalinin, S. V.; Jesse, S.; Liu, W.; Balandin, A. A. *Appl. Phys. Lett.* **2006**, *88*, 153902-3.